Article ID: 1000-324X(2015)09-0995-07 **DOI:** 10.15541/jim20150163

High Ion Conductivity in Garnet-type F-doped $Li_7La_3Zr_2O_{12}$

LIU Cai, WEN Zhao-Yin, RUI Kun

(CAS Key Laboratory of Materials for Energy Conversion, Shanghai Institute of Ceramics, Chinese Academy of Sciences, Shanghai 200050, China)

Abstract: A novel garnet-type solid electrolyte, F-doped $Li_7La_3Zr_2O_{12}$ (LLZO), was prepared *via* conventional solid-state reaction. Certain fluoride compounds were known to form the pure cubic garnet structure after continuous calcination at 900℃ and 1125℃, seperately. Fluorine ions doped in LLZO contributed to the stabilization of high ion conductivity garnet phase as well as the enhancement of sintering activity. The effects of fluorine ions were studied using the dopants LiF and CaF_2. The 1.0wt% LiF-LLZO samples exhibited a total conductivity of 5×10^{-4} S/cm close to the bulk conductivity value of un-doped LLZO, while its activation energy was 0.26 eV, lower than that of other cation-doped LLZO samples. The strong intensity of the peaks indexed to (321), (400), (642), and (800) in XRD patterns indicated the growth of ceramic grains of F-doped LLZO in certain favorable crystallographic orientations during sintering process. In addition, a unique microstructure was revealed in the novel garnet-type oxide pellets, showing the grain boundary almost removed and closed pores formed, which resulted in the negligible grain boundary and the high total ion conductivity.

Key words: solid electrolyte; garnet-type; fluorine ion doping; microstructure

Recently, green energy conversion and storage systems have attracted much attention in both academia and industry in consequence of global warming and fossil fuel crisis[1]. Solid electrolytes, also known as fast ion conductors, can be used in energy storage devices such as solid oxide fuel cells and lithium-ion batteries. The solid electrolyte permits movement of ions without the need for a soft membrane or liquid separating the electrodes. In a lithium-ion battery, for example, lithium ions move from the negative electrode to the positive electrode during discharge (and back when charging) *via* the solid electrolyte which can conduct lithium ions through vacancies in the electrolyte crystal lattice. Moreover, the solid electrolyte can also provide a hermetic barrier between the anode and the cathode in order to prevent them from sharing a common electrolyte solution. As the key component, a good solid electrolyte should contain the generalized properties such as high ionic conductivity at ambient temperature, negligible electronic conductivity, a negligibly small grain-boundary resistance, wide electrochemical window, inertia to other cell components, environment-friendliness, non-toxic, non-hygroscopic and low cost[2]. However, some problems can be found in the applications of the state-of-art solid electrolytes. For example, due to the high hygroscopic nature, the sulphide electrolyte (*e.g.* glass ceramic Li_2O-P_2S_5) releases the toxic H_2S in air or moisture environment. Its stability against the high voltage cathode materials is also in dispute[3]. Besides, the Ti-based materials, such as NASICON- type structure phosphates $LiTi_2P_3O_{12}$ and A-site deficient perovskite-type oxides $(Li,La)TiO_3$, suffer from electrochemical instability because of the reduction of Ti^{4+} to Ti^{3+}. To date, no solid electrolyte has been in practical use[4].

A lithium garnet-type oxide with the chemical composition of $Li_7La_3Zr_2O_{12}$(LLZO), firstly reported by Thangadurai, *et al* in 2007, is considered as a promising solid electrolyte for its high ion conductivity, chemical stability *vs* metal Li and wide electrochemical potential window[5-6]. The cubic phase of LLZO exhibits the lithium ion conductivity as high as 10^{-4} S/cm, which is two orders of magnitude higher than that of the tetragonal phase. In the framework of cubic garnet phase, La ions are located in the 8-coordinantion site and Zr ions are located in the octahedral site, while the Li can present at the tetrahedral site and the octahedral site. The opposing faces of the octahedron are shared with the adjacent tetrahedral LiO_4 units. In

Received date: 2015-04-07; **Modified date:** 2015-04-17; **Published online:** 2015-06-10
Foundation item: National Natural Science Foundation of China(51373195, 51272267, 51432010); Key Fundamental Research Project from Science and Technology Commission of Shanghai Municipality(14JC1493000)
Biography: LIU Cai(1987–), male, candidate of PhD degree. E-mail: liucai@student.sic.ac.cn
Corresponding author: WEN Zhao-Yin, professor. E-mail: zywen@mail.sic.ac.cn

this connecting mode, the three-dimensional network structure is built up for fast lithium ion conduction, as illustrated in Fig. 1(a). Therein, the migration of lithium ion should refer to the comfortable local rearrangement depending on the occupancy of the two possible lithium sites[7]. Hence, subsequent research work has been centered on the tailoring of this ceramic material for its further application in solid-state batteries. In order to obtain higher conductivity, abundant aliovalent cation substitutions have been explored to modify the migrating path and lithium ion population accompanying with the rearrangement of Li sites occupancy, such as $Li_{7-y}La_3Zr_{2-x}M_xO_{12}$ (M=Al, Ga, Y, Sb, Si, Ge, Nb, Ta, Te)[3-4, 8-14]. Although the conductivity of some other conductors was also significantly improved by anion substitutions, it has not been applied in the garnet-type lithium ion conductor[15-16]. At present, the total conductivity of the most prospective garnet-type electrolyte LLZO was 3×10^{-4} S/cm and the bulk conductivity was over 5×10^{-4} S/cm at room temperature, which indicated that the contribution of grain boundary to the total resistance was more than 40%[5]. So it is necessary to design the modified grain boundary to improve the lithium ionic conductivity or the ceramic density of lithium garnet-type oxides. Besides, the availability of dense, solid, ion-conductive electrolyte membranes is important to the development of Li-ion batteries. A challenge in the formation of such membranes *via* traditional ceramic routes is the inability to sinter suitable starting materials to sufficient density to form a membrane which is hermetic while providing the requisite conductivity and economy. Herein, we found that the ion conductivity of the LLZO was close to the bulk conductivity by adding some fluorine component while the grain boundary was almost removed. Besides, a new kind of ceramic containing only closed pores in microstructure was obtained, which can work as the hermetic electrolyte even when the density was not very high.

1 Experiment

Lithium carbonate (AR), zirconium oxide(AR), lanthanum oxide(99.99%), lithium fluoride(CP) and calcium fluoride(99.99%), aluminum oxide(AR) were used as the initial reagents to prepare the garnet-type oxides *x*wt% LiF-LLZO, 1.5wt%CaF_2-LLZO and 2wt%Al_2O_3-LLZO, wherein *x* was equal to 0, 0.5, 1, 2, 5 in weight percentage, and each composition was represented as un-doped LLZO, 0.5LF-LLZO, 1.0LF-LLZO, 2.0LF-LLZO, 5.0LF-LLZO, 1.5CF-LLZO and 2Al-LLZO, respectively. 10wt% excess of Li_2CO_3 was added to compensate the lithium loss during the sintering process. The traces of moisture and adsorbed CO_2 were removed from lanthanum oxide by heat treatment at 900℃ for 12 h. The raw materials with the stoichiometry ratio were mixed together *via* a wet grinding process in which the ethanol and zirconium balls were used as the milling media. The mixtures of reactants were calcinated at 900℃ and 1125℃ in an alumina crucible, following the ball-milling process mentioned above. Then the synthesized powder was dried and pressed into the green pellets. The pellets were sintered at 1230℃ for 36 h covered with the mother powder at all sides.

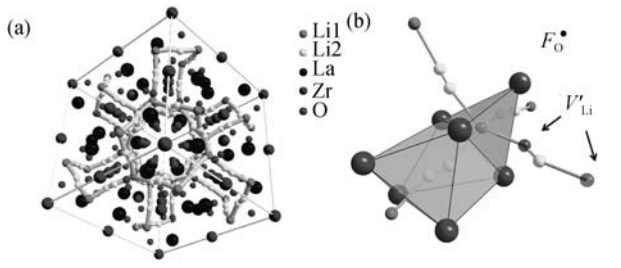

Fig. 1 Crystal structure for the cubic LLZO
(a) Three-dimensional migration structure of lithium ion viewed in (111) orientation; (b) F substitution in oxide polyhedral structure model

Powder X-ray diffraction (PXRD, Rigaku, Ultima IV, nickel-filtered Cu-Kα radiation, λ=0.1542 nm) was employed to determine the phase formation of synthesized powder or pellets at room temperature in the 2θ range of 10°~ 80° with the step of 0.1°/s. The cross-section microstructure morphologies and the main elements of the ceramic pellets were revealed by the scanning electron microscopy with the energy dispersive detector (Hitachi, S-3400N).

The ionic conductivity was measured at room temperature by the AC impedance analysis (Autolab, Model PGSTAT302N). The potentiostatic impedance model of frequency resistance analysis was selected as the test model, while the frequency ranged within 1 Hz to 1 MHz and the electrical perturbation was set to 20 mV. The ceramic pellets were polished after the sintering process. The thickness of the pellets was less than 1.5 mm and the diameter was about 9~11 mm. Before the measurement, both the parallel surfaces were sputtered with gold as the lithium ion blocking electrode. The activation energy was measured at the temperature range of 298 K to 423 K in a temperature chamber.

2 Results and discussions

A series of *x*wt% LiF-LLZ powder were synthesized by traditional solid-state reaction. The XRD patterns of the un-doped LLZO, 0.5F-LLZO, 1.0F-LLZO, 2.0F-LLZO and 5.0F-LLZO were shown in Fig. 2, compared with the pattern of the cubic garnet-type LLZ calculated from the reference structure[17]. The diffraction peaks of F-doped LLZO exhibited good in crystallinity while the positions

and relative intensities coincided with the calculated data except that of un-doped LLZO. For all the fluorine doped LLZO samples, a cubic garnet structure belonging to the $Ia\bar{3}d$ space group was obtained after two-step calcination But the un-doped LLZO phase just has a predominant tetragonal symmetry ($I4_1acd$ space group), which was characterized by the splitting peaks, in accordance with the previous conclusion reported about the Al-free LLZO[18]. However, based on the XRD results, the doped fluorine ions were also beneficial for stabilizing the cubic phase, which indicated that the F-doped LLZO is an analogue to the pure cubic LLZO. Figure 1(b) depicted fluorine ion substitution in the garnet crystal structure, which could be represented by $Li_{7-x}La_3Zr_2O_{12-x}F_x$. At the lower dopant levels, the incorporation of F may influence the number fraction of Li vacancies and, thus, the Li ion conductivity. At the same time, it helped to release disorder of the octahedral lithium sites, possibly resulting in stability of cubic garnet phase at room temperature. It has been reported that the pure cubic garnet phase of Ce-doped yttrium aluminum garnet phosphor was synthesized with the LiF assistance at a lower temperature[19]. Both results demonstrated that fluorine doping might play another key aspect in stabilizing the cubic garnet phase. However, at the high levels of the LiF dopants above 2.0wt%, the XRD pattern showed the distinct impurity phase which was indexed to $La_2Zr_2O_7$ with the pyrochlorite structure. The intensity of impurity peaks were strengthened with increasing LiF content. Except the individual peaks of $La_2Zr_2O_7$ at 28° and 33°, the overlapping peaks of $La_2Zr_2O_7$ and garnet LLZO were at 47° and 56°, which respectively corresponded to the (631) and (800) crystallographic planes of cubic garnet.

In order to further study the effect of fluorine ion in sta

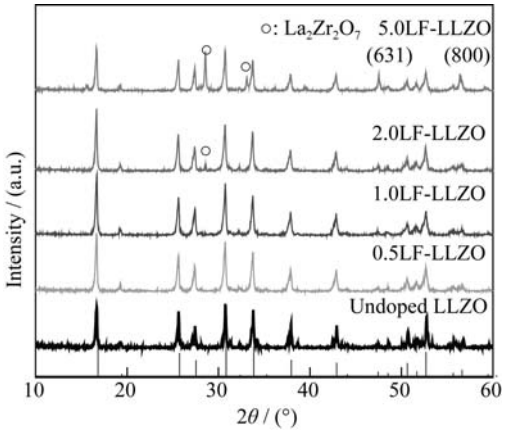

Fig. 2 XRD patterns of synthesized LLZO powder doped with different amounts of LiF after two-step calcinations

The impurity peaks were indexed to the $La_2Zr_2O_7$ with niobpyrochlore structure. The red vertical lines at the bottom represent the calculated peak positions and intensities for cubic LLZ[17]

bilizing the cubic garnet phase, samples of 1.5CF-LLZOand 2Al-LLZO were also prepared under the same conditions. The mole content of fluorine ion doped in LLZO was the same for 1.5CF-LLZO and 1.0F-LLZO. The XRD pattern of 1.5CF-LLZO after two-step calcination was shown in the Fig. 3, compared with those of un-doped LLZO, 1.0F-LLZO and 2Al-LLZO. The calcinations were carried out in the alumina crucibles, which implied that a certain amount of Al might be introduced in the products by the reaction between lithium carbonate and the crucible. Nevertheless, the content was not high enough to transform the precursors into the cubic phase completely. So the major composition of un-doped LLZO was still maintained as tetragonal phase. When additional Al was introduced in LLZO, just like 2Al-LLZO, the cubic garnet phase would be obtained at room temperature. Each peak of 1.5CF-LLZO and 2Al-LLZO powder matched with the cubic garnet structure successfully. The influence of excess lithium, which was introduced by LiF, was examined by comparing with the results of 1.5CF-LLZO. The F-based compounds with different cations confirmed that the fluorine ion substitution in lithium garnet-type oxides would stabilize the cubic garnet phase just as what the aliovalent Al ion substitutions had achieved.

The powder of pure garnet phase was compacted into pellets and then subjected to 200 MPa pressure by the cool isostatic pressing. All sides around the pellet was covered by the mother powder and sintered at 1230℃ for 36 h in a sealed platinum capsule, which would not only minimize the evaporation of lithium but also prevent the strong reaction between the pellet and aluminum crucible during the sintering process. After the high temperature sintering process, the pellets were polished to be less than 1.5 mm thick to remove the section with non-uniform composition. The abnormally high intensity peaks indexed to (321), (400), (642) and (800) were observed in the XRD pattern of 1.0F-LLZO as shown in Fig. 4. This signified that the

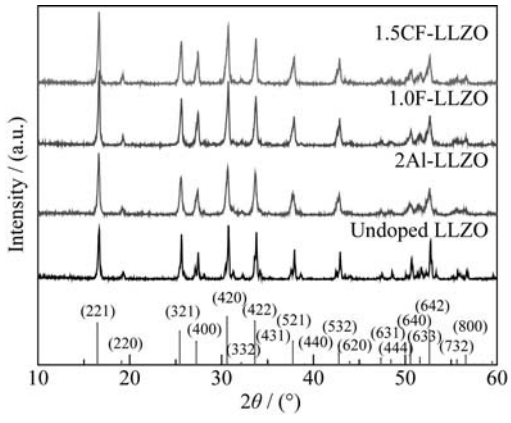

Fig. 3 XRD patterns of synthesized LLZO powder with different fluorides after two-step calcination

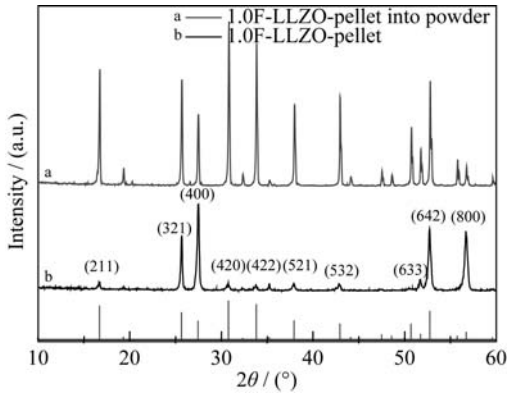

Fig. 4 XRD patterns of 1.0F-LLZO sintered pellet and powder
The typical peaks of cubic garnet phase were indexed for illustration

ceramic grains were grown in some favorable crystallo graphic orientations during the sintering process. However, normal relative intensity peaks were recovered after the pellet was crashed into powder, which is the same case in CF-doped system as well. The phenomenon suggested that the ceramic pellet might gradually deviate from the polycrystalline ceramic into a probable single crystal via the long sintering process. Besides, the grain boundary might dissolve step by step.

Figure 5 showed the Nyquist plots of 1.0F-LLZO, 0.5F-LLZO, 2Al-LLZO and 1.5CF-LLZO samples at room temperature measured in air. All the polished samples were sputtered with Au as the Li-ion blocking electrodes. In Fig. 5(a), no semicircle of the bulk impedance was observed at the high frequency region for fluorine doped LLZO samples except the turning point. At the low frequency region, a tail representing the electrode resistance was observed, which suggested that the electrode block mobile lithium ions. Similar shape of the plots was also found in other reports for the cations doped garnet electrolytes[8, 11, 20-21]. The semicircle corresponding to the grain-boundary impedance was revealed in the plots only for the 2Al-LLZO samples. The undetected grain boundary for 0.5F-LLZO and 1.0F-LLZO samples implied that the small grain-boundary impedance might be negligible as compared to the bulk impedance. The phenomenon was also found in the high density LLZO sample prepared by the hot-press method[18, 22]. As a result, the total conductivity of the 0.5F-LLZO and 1.0F-LLZO samples was estimated from the intercept in low frequency on the Z' axis and the samples dimensions. The calculated values were 4.5×10^{-4} S/cm and 5×10^{-4} S/cm, respectively, which approached the bulk conductivity of un-doped LLZO[5]. Meanwhile, the total conductivity of 1.5CF-LLZO was calculated to be 5×10^{-5} S/cm from Fig. 5(b) *via* the same way, which was much lower than that of un-doped LLZO. It had proved that the alkaline rare earth metal ions could substitute the lanthanum ions in the garnet crystal structure[23-25]. As for the $Li_6CaLa_2Nb_2O_{12}$ garnet electrolyte, Thangadurai *et al*[24]. had reported that the total conductivity was about 1.6×10^{-6} S/cm (22℃) and the grain-boundary resistance contribution was about 27% of the total resistance. As a result of the Ca^{2+} substitution, the total conductivity of the $Li_5La_3Nb_2O_{12}$ decreased from 8×10^{-6} S/cm to 1.6×10^{-6} S/cm, which occurred in Ca-doped LLZO as well, though the grain-boundary contribution was removed by the function of fluorine ion. In Fig. 5(c), a clear semicircle representing the grain-boundary resistance was observed in the plot of 2Al-LLZO samples. The solid line represented fitted data based on the equivalent circuit model consisting of parallel resistance (R) and constant phase element (CPE) contributions R_b(R1CPE1)(R2CPE2), where b, 1 and 2 denoted the bulk, grain boundary and electrode, respectively. The total conductivity of 2Al-LLZO samples reached 2×10^{-4} S/cm, while the

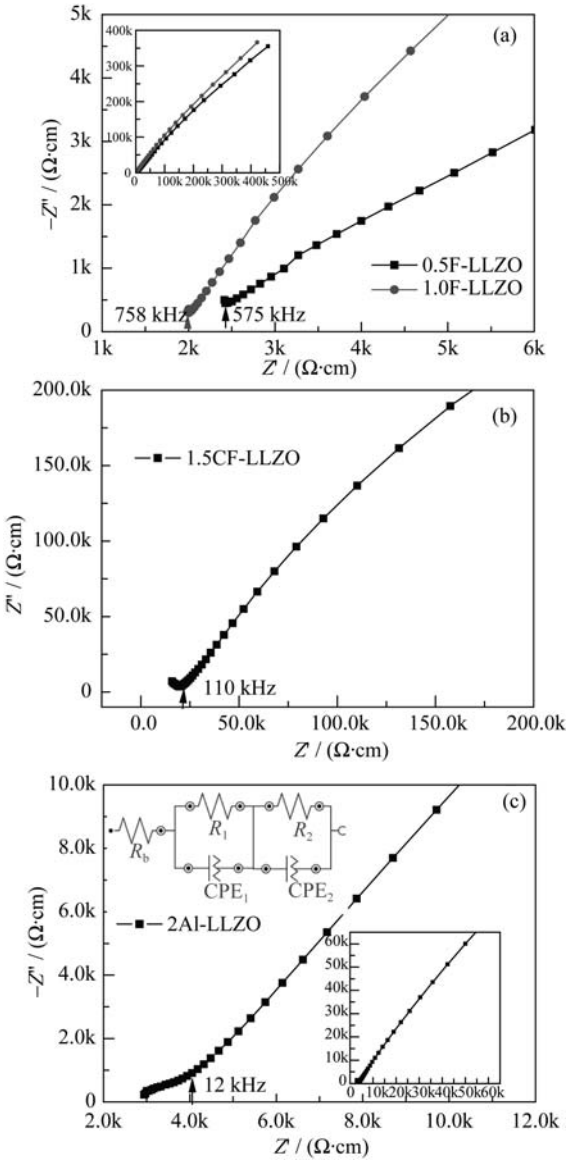

Fig. 5 AC impedance plots at room temperature
(a) 0.5F-LLZO and 1.0LLZO; (b) 2Al-LLZO; (c) 1.5CF-LLZO

grain boundary resistance contribution was about 28%. Based on the comparison of anion and cation doped garnet electrolytes, fluorine ions exhibited great advantages in improving the total ion conductivity by lowering the grain boundary contributions.

Figure 6 showed the total conductivity as a function of 1000/T for the sample of 1.0F-LLZO. The temperature dependence of the ion conductivity was expressed by the Arrhenius equation.

$$\sigma T = A\exp(-E_a / kT) \quad (1)$$

The activation energy for the total conductivity was calculated to be 0.26 eV, which was smaller than that in $Li_7La_3Zr_2O_{12}$ (0.30 eV), Ta-doped LLZO (0.35 eV), Nb-doped LLZO (0.47 eV) and other cations-doped LLZO, but comparable to the hot-press Al-doped LLZO (0.26 eV)[4-5, 8, 18]. The low activation energy was ascribed to the negligible grain boundary impedance, which was suggested by Rangasamy, *et al* and Ban, *et al*[18, 26].

To further confirm the results above, the cross-section microstructure morphologies of the ceramic pellets of 0.5F-LLZO, 1.0F-LLZO, 1.5CF-LLZO and 2Al-LLZO were revealed by the scanning electron microscope (SEM), which were shown in Fig. 7. As to the SEM image of the 0.5F-LLZO ceramic pellet shown in Fig. 7(a), large closed pores were observed in the cross-section of the pellet, the size of which was even as large as 30 μm. Nevertheless, the pores of the 1.0F-LLZO ceramic pellet in Fig. 7(b) were comparatively much smaller, just 10 μm. The formation of close pores might be due to the evaporation of lithium oxide and subsequent shrinkage during grain growth[27]. For the 1.5CF-LLZO pellet in Fig. 7(c), the morphology was much different from that of lithium fluoride doping LLZO whereas the liquid phase was also generated during the sintering process. The homogeneous microstructure prove that the grain boundary disappeared because of the influence of fluoride compounds, which contributed to the high ion conductivity and low activation energy of fluorine doped LLZO. However, the special

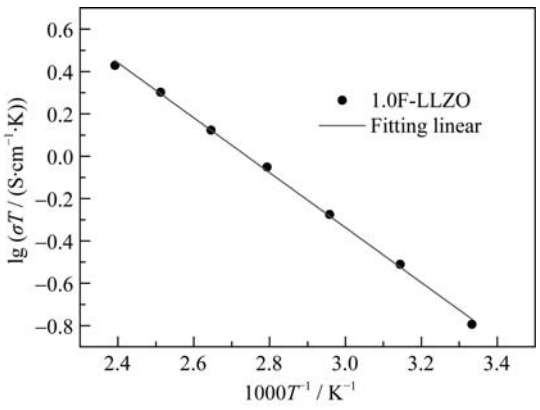

Fig. 6 Temperature dependence of the lithium conductivity of 1.0F-LLZO and the Arrhenius plot linear-fitting results

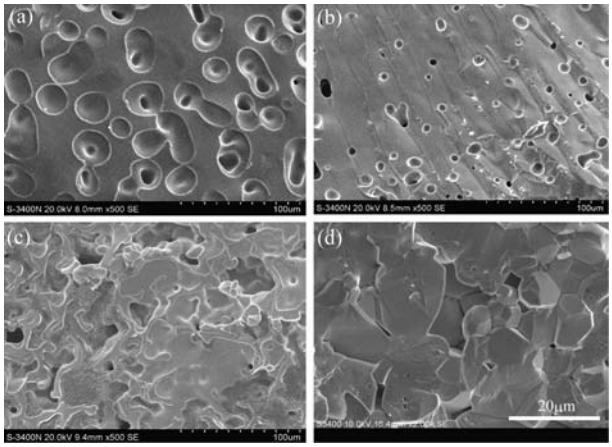

Fig. 7 The SEM images of cross-section microstructure for LLZO doped with different fluoride compounds
(a) 0.5F-LLZO; (b) 1.0F-LLZO; (c) 1.5CF-LLZO; (d) 2Al-LLZO

microstructure was much different from other doping LLZO solid electrolytes. Clear grain boundary was observed in the microstructure of 2Al-LLZO in Fig. 7(d), which led to the 28% grain-boundary resistance contribution. Furthermore, the appearance of the decentral closed pores in the ceramic pellets might restrain the chemical etching of the interface with polar solutions and the growth of lithium dendrite, which would be beneficial to the long-term performance of lithium batteries. The unique microstructure with closed pores might be ascribed to the enhancement of sintering activity of LLZO by the incorporation of fluoride compounds.

3 Conclusions

A new kind of garnet-type electrolyte was prepared by conventional solid-state reaction, which was presented by the formula $x$wt%LiF-$Li_7La_3Zr_2O_{12}$ ($0<x<2$). The incorporation of certain amount of fluoride compounds assists the formation of pure cubic garnet phase at room temperature. It was found that grains in the ceramic pellet grew in some favorable crystallographic orientations ((321), (400), (642) and (800)) for the F-doped LLZO during the sintering process. The total conductivity of 1.0F-LLZO samples was found to be 5×10^{-4} S/cm which approached the bulk conductivity of un-doped LLZO, while its activation energy was 0.26 eV and lower than other cation-doped LLZO. In addition, a special microstructure was revealed in the new kind of garnet-type oxide pellets. The grain boundary was almost removed and the closed pores were formed in the ceramic microstructure, which contributed to the negligible grain boundary and high total ion conductivity.

Acknowledgements We thank Prof. Chowdari B V R (Department of Physics, National University of Singapore) for helpful discussion.

References:

[1] CUSSEN E J, YIP T W S, O'NEILL G, *et al*. A comparison of the transport properties of lithium-stuffed garnets and the conventional phases $Li_3Ln_3Te_2O_{12}$. *J. Solid State Chem.*, 2011, **184(2):** 470–475.

[2] KNAUTH P. Inorganic solid Li ion conductors: an overview. *Solid State Ionics*. 2009, **180(14/15/16):** 911–916.

[3] ADAMS S, RAO R P. Ion transport and phase transition in $Li_{7-x}La_3(Zr_{2-x}M_x)O_{12}$ (M = Ta^{5+}, Nb^{5+}, x=0, 0.25). *J. Mater. Chem.*, 2012, **22(4):** 1426–1434.

[4] OHTA S, KOBAYASHI T, ASAOKA T. High lithium ionic conductivity in the garnet-type oxide $Li_{7-x}La_3(Zr_{2-x}, Nb_x)O_{12}$ (x=0-2). *Journal of Power Sources*, 2011, **196(6):** 3342–3345.

[5] MURUGAN R, THANGADURAI V, WEPPNER W. Fast lithium ion conduction in garnet-type $Li_7La_3Zr_2O_{12}$. *Angew Chem-Int Edit.*, 2007, **46(41):** 7778–7781.

[6] BUSCHMANN H, DOLLE J, BERENDTS S, *et al*. Structure and dynamics of the fast lithium ion conductor "$Li_7La_3Zr_2O_{12}$". *Physical Chemistry Chemical Physics*, 2011, **13(43):** 19378–19392.

[7] CUSSEN E J. Structure and ionic conductivity in lithium garnets. *J. Mater. Chem.*, 2010, **20(25):** 5167–5173.

[8] LI Y T, HAN J T, WANG C A, *et al*. Optimizing Li^+ conductivity in a garnet framework. *J. Mater. Chem.*, 2012, **22(30):** 15357–15361.

[9] HUANG M, DUMON A, NAN C W. Effect of Si, In and Ge doping on high ionic conductivity of $Li_7La_3Zr_2O_{12}$. *Electrochem. Commun.*, 2012, **21:** 62–64.

[10] MURUGAN R, RAMAKUMAR S, JANANI N. High conductive yttrium doped $Li_7La_3Zr_2O_{12}$ cubic lithium garnet. *Electrochem. Commun.,* 2011, **13(12):** 1373–1375.

[11] KUMAZAKI S, IRIYAMA Y, KIM K H, *et al*. High lithium ion conductive $Li_7La_3Zr_2O_{12}$ by inclusion of both Al and Si. *Electrochem. Commun.*, 2011, **13(5):** 509–512.

[12] EL SHINAWI H, JANEK J. Stabilization of cubic lithium-stuffed garnets of the type "$Li_7La_3Zr_2O_{12}$" by addition of gallium. *Journal of Power Sources*, 2013, **225:** 13–19.

[13] DEVIANNAPOORANI C, DHIVYA L, RAMAKUMAR S, *et al*. Lithium ion transport properties of high conductive tellurium substituted $Li_7La_3Zr_2O_{12}$ cubic lithium garnets. *Journal of Power Sources*, 2013, **240:** 18–25.

[14] CAO Z Z, REN W, LIU J R, *et al*. Microstructure and ionic conductivity of Sb-doped $Li_7La_3Zr_2O_{12}$ ceramics. *Journal of Inorganic Materials*, 2014, **29(2):** 220–224.

[15] LI J X, WEN Z Y, XU X X, *et al*. Lithium-ion conduction in the anion substituted $La_{2/3-x}Li_{3x-y}TiO_{3-y}F_y$ electrolyte with perovskite-type structure. *Solid State Ionics*. 2005, **176(29/30):** 2269–2273.

[16] OKUMURA T, YOKOO K, FUKUTSUKA T, *et al*. Improvement of Li-ion conductivity in A-site disordering lithium-lanthanum-titanate perovskite oxides by adding LiF in synthesis. *Journal of Power Sources*, 2009, **189(1):** 536–538.

[17] GEIGER C A, ALEKSEEV E, LAZIC B, *et al*. Crystal chemistry and stability of "$Li_7La_3Zr_2O_{12}$" garnet: a fast lithium-ion conductor. *Inorg. Chem.*, 2011, **50(3):** 1089–1097.

[18] RANGASAMY E, WOLFENSTINE J, SAKAMOTO J. The role of Al and Li concentration on the formation of cubic garnet solid electrolyte of nominal composition $Li_7La_3Zr_2O_{12}$. *Solid State Ionics*, 2012, **206:** 28–32.

[19] JIAO H, MA Q, HE L L, *et al*. Low temperature synthesis of YAG:Ce phosphors by LiF assisted Sol-Gel combustion method. *Powder Technol.*, 2010, **198(2):** 229–232.

[20] GUPTA A, MURUGAN R, PARANTHAMAN M P, *et al*. Optimum lithium-ion conductivity in cubic $Li_{7-x}La_3Hf_{2-x}Ta_xO_{12}$. *Journal of Power Sources*, 2012, **209:** 184–188.

[21] TADANAGA K, TAKANO R, ICHINOSE T, *et al*. Low temperature synthesis of highly ion conductive $Li_7La_3Zr_2O_{12}$–Li_3BO_3 composites. *Electrochem Commun.*, 2013, **33:** 51–54.

[22] KOTOBUKI M, MUNAKATA H, KANAMURA K, *et al*. Compatibility of $Li_7La_3Zr_2O_{12}$ solid electrolyte to all-solid-state battery using Li metal anode. *J. Electrochem. Soc.*, 2010, **157(10):** A1076–A1079.

[23] THANGADURAI V, WEPPNER W. $Li_6ALa_2Ta_2O_{12}$(A=Sr, Ba): novel garnet-like oxides for fast lithium ion conduction. *Advanced Functional Materials.*, 2005, **15(1):** 107–112.

[24] THANGADURAI V, WEPPNER W. $Li_6ALa_2Nb_2O_{12}$ (A = Ca, Sr, Ba): a new class of fast lithium ion conductors with garnet-like structure. *J. Am. Ceram. Soc.*, 2005, **88(2):** 411–418.

[25] KIHIRA Y, OHTA S, IMAGAWA H, *et al*. Effect of simultaneous substitution of alkali earth metals and Nb in $Li_7La_3Zr_2O_{12}$ on lithium-ion conductivity. *ECS Electrochem Lett.*, 2013, **2(7):** A56–A59.

[26] BAN C W, CHOI G M. The effect of sintering on the grain boundary conductivity of lithium lanthanum titanates. *Solid State Ionics*, 2001, **140(3/4):** 285–292.

[27] HUANG M, SHOJI M, SHEN Y, *et al*. Preparation and electrochemical properties of Zr-site substituted $Li_7La_3(Zr_{2-x}M_x)O_{12}$ (M = Ta, Nb) solid electrolytes. *Journal of Power Sources*, 2014, **261:** 206–211.

高电导率 F 掺杂 $Li_7La_3Zr_2O_{12}$ 石榴石结构固体电解质

刘 才, 温兆银, 芮 琨

(中国科学院 上海硅酸盐研究所, 中国科学院能量转换材料重点实验室, 上海 200050)

摘 要: 通过传统固相反应法合成一种新型的F掺杂$Li_7La_3Zr_2O_{12}$ (LLZO)石榴石结构固体电解质。添加适量LiF和CaF_2等氟化物经过两步煅烧在室温下获得纯立方相的 LLZO 陶瓷粉体, 验证氟离子掺杂具有稳定石榴石结构立方相和增强陶瓷烧结活性的作用。制备的 1wt% LiF-LLZO 电解质总电导率达 5×10^{-4} S/cm, 接近立方相 LLZO 的体电导率, 电导活化能仅为 0.26 eV, 低于其他阳离子掺杂的 LLZO。(321)、(400)、(642)和(800)晶面衍射峰由于晶粒的生长取向而显著增强, 陶瓷内部晶界消失, 形成由闭气孔构成的独特显微结构, 导致该新型电解质的晶界阻抗的消失和总电导率的提升。

关 键 词: 固体电解质; 石榴石结构; 氟离子掺杂; 显微结构

中图分类号: TM911 **文献标识码:** A